We are IntechOpen, the world's leading publisher of Open Access books Built by scientists, for scientists

6,900
Open access books available

185,000
International authors and editors

200M
Downloads

Our authors are among the

154
Countries delivered to

TOP 1%
most cited scientists

12.2%
Contributors from top 500 universities



WEB OF SCIENCE™

Selection of our books indexed in the Book Citation Index in Web of Science™ Core Collection (BKCI)

Interested in publishing with us?
Contact book.department@intechopen.com

Numbers displayed above are based on latest data collected.
For more information visit www.intechopen.com



Chapter 8

Controlled Functionalization of Graphene Layers

Maurizio Galimberti, Vincenzina Barbera and

Annalisa Sironi

Additional information is available at the end of the chapter

http://dx.doi.org/10.5772/67630

Abstract

Controlled functionalization of graphene layers is one of the most important research objectives in the material chemistry. A well established procedure is the oxidation with strong acids and oxidizing agents often in harsh and dangerous reaction conditions giving products of unknown precise structure. In this chapter, the controlled functionalization of graphene layers with a derivative of serinol is presented, avoiding toxic reagents and dangerous reaction conditions. The derivative is the bio-based serinol pyrrole, obtained through the neat reaction of serinol with 2,5-hexanedione; the graphitic substrate was high surface area graphite (HSAG) with high-shape anisotropy. The functionalization reaction, characterized by a 85% atomic efficiency (water is the only by-product), evolved with high yields leading to functionalized graphene layers through the controlled introduction of oxygen and nitrogen-containing functional groups. Sustainable processes were adopted, such as ball milling and heating. The mechanism pathway, the characterization of HSAG and reaction products through a wide range of analytical methods, some successful applications of the adducts are discussed in this chapter. The functionalization left the bulk crystalline structure of the layers substantially unaltered. Stable dispersions in water and eco-friendly solvents were prepared.

Keywords: graphene, functionalization, serinol derivative

INTECH
open science | open minds

© 2017 The Author(s). Licensee InTech. This chapter is distributed under the terms of the Creative Commons Attribution License (http://creativecommons.org/licenses/by/3.0), which permits unrestricted use, distribution, and reproduction in any medium, provided the original work is properly cited. CC BY

1. Introduction

Graphene [1–3] is the thinnest material on Earth and is commonly considered as a single layer of graphite. It has a two-dimensional conjugated structure, good thermal stability, very high aspect ratio and specific surface area and has, as a consequence, outstanding electronic, thermal and mechanical properties. At low temperatures and high magnetic fields, quantum Hall effect has been observed in graphene layers for both electrons and holes [4, 5]. The in-plane thermal conductivity of graphene is among the highest recorded for known materials, about 2000–4000 W m^{-1} K^{-1} at room temperature [6, 7]. A graphene sheet has theoretical elastic modulus of over 1 TPa and Young modulus of about 1060 MPa [8, 9].

In the light of such properties, impressive research activity is currently carried out for applying graphene in high-performance materials [10], in fields such as nanoelectronics [3], energy storage and energy conversion [11]. Graphene composites allow contributing the exceptional properties of graphene to the macroscopic scale. In particular, light, flexible, robust and conductive graphene papers find a broad spectrum of applications such as electrochemical energy storage devices [12], catalyst supports and fuel cells [13], sensors and actuators [14], chemical filters and membranes [15] and structural composites [16].

Graphene and derivatives are also finding increasing applications in the field of catalysis [17, 18]. Indeed, carbocatalysis is largely used for promoting synthesis and transformation of organic or inorganic substrates: carbons favour reduction, oxidation and bond-forming reactions [19].

All the applications mentioned above become successful if graphene or graphitic aggregates made by only few layers of graphene can be used. Large research efforts are thus made in order to prepare graphene and few-layer graphene [3, 10, 20–23].

Moreover, high interest is on functionalization of graphene layers [24–33]. Graphene oxide is considered a stable carbon framework to be functionalized [24] and, as it will be discussed in the next paragraph, is the product of the first step of the oxidation-reduction process aimed at preparing graphene starting from graphite. It is thus the subject of much of the research on functionalization [24–26].

In our group, research was performed with the following objectives:

(i) To prepare graphene and few-layer graphene through a simple, environmentally friendly, sustainable and economically viable method that could be applied for large-scale development

(ii) To introduce functional groups on graphene layers, containing in particular heteroatoms such as oxygen and nitrogen

(iii) To preserve the ideal structure of graphene, in graphene and functionalized graphene layers.

In a nutshell, our main goal was the controlled functionalization of graphene layers.

The present chapter summarizes the results of such a research.

http://dx.doi.org/10.5772/67630

2. Preparation of graphene and functionalized graphene: prior art

In the light of what is reported in Section 1, it can be easily understood that primary objectives of the research in the field of graphene are as follows:

(i) To prepare graphene or graphitic nanofillers made by only few layers of graphene, through a simple method, suitable for large-scale production

(ii) To preserve the ideal graphene structure.

Nowadays, single-layer or few-layer graphene are obtained through bottom-up and top-down approaches [3, 10, 20–23], such as epitaxial growth of graphene films, micromechanical cleavage and dilution in appropriate solvents.

Best practice, particularly in view of large scale applications, is considered the oxidation of graphite or graphitic nanofiller to graphite oxide (well known as GO), followed by thermal or chemical reduction. However, such a pathway is affected by several flaws, in the oxidation and reduction steps and also in consideration of the features of reduced GO.

Harsh and even dangerous reaction conditions are required for the oxidation of pristine graphitic material. First papers on carbon oxidation date back to the nineteenth century. Brodie reported the use of fuming HNO_3 and $KClO_3$ as intercalant and oxidant [34], in the frame of a multicycle process, that produced toxic and explosive gases such as NO_2/N_2O_4 and ClO_2, respectively. Indeed, explosions have been documented [35, 36]. Towards the end of the century, Staudenmeier used a blend of H_2SO_4 and HNO_3 (2/1) with $KClO_3$ as oxidant, in a one-step process that still produced explosive ClO_2 [37]. These methods of the eighteenth century cannot be taken into consideration for large-scale production of GO. Towards the 1960s of the last century, Hummers reported the use of $H_2SO_4/NaNO_3$ and $KMnO_4$ to intercalate and oxidize graphite [38]. The Hummers' method is considered promising for large-scale production of GO as $KMnO_4$ is very efficient and reaction takes only few hours, explosive ClO_2 is not formed and the replacement of HNO_3 with $NaNO_3$ eliminates acidic smokes. However, NO_2/N_2O_4 are still formed and reaction products such as manganese ions can be hardly removed, only by washing with acids such as HCl which, in turn, remains strongly absorbed on the graphitic substrate. Finally, only partial oxidation is obtained [39–41]. Research has been thus dedicated to improve the Hummers' method [40–43]. $NaNO_3$ has been removed by increasing the amount of $KMnO_4$ and by using a H_2SO_4/H_3PO_4 mixture [40]. $NaNO_3$ has been simply removed, without observing negative effects on the reaction [41]. However, only an incomplete conversion of graphite to GO was obtained. The pre-oxidation of graphite with P_2O_5 and $K_2S_2O_8$ in H_2SO_4 adds a further step [44]. The complete conversion to GO has been reported [42] by using graphite flakes with sizes in the range of 3–20 μm. In another variation of the Hummers' method, the concentration of $NaNO_3$ and $KMnO_4$ and the residence times have been modified [43]. GO can be also prepared by solvent-free mechanochemical oxidation of graphite [45]. However, such a method can be hardly employed for large-scale production.

The Hummers' method based on the use of $NaNO_3$, applied by one of the authors of the present chapter is fully described in Ref. [46].

It is evident that the objective of developing a really simple method, suitable for large-scale production, has not been achieved yet.

The reduction step is crucial in order to obtain graphene. Well-known methods are based on the use of hydrazine [47–50] or hydrogen plasma [49]. To avoid reaggregation of graphitic flakes, a stabilizing agent should be added [9, 51]. Hydrazine is well known as a toxic reagent. Hence, eco-friendly methods have been attempted. Quick deoxygenation of graphite oxide assisted by a base (NaOH, 0.1 M) has been performed at moderate temperatures (80°C) [52]. Ascorbic acid has been used as well [53]. Thermal [54] and flash [55] reductions have been reported.

However, it is widely acknowledged that reduction is still incomplete and that the ideal graphene structure is neither preserved nor restored [20, 56]. Hence, also this objective is not achieved yet.

However, the pathway that could lead to graphene through graphite oxidation gives the opportunity of preparing GO that could be a suitable building block for further reactions [24–26] as well as for catalytic applications [17, 18]. Moreover, functionalized single-layer graphene sheets can be prepared by splitting graphite oxide [57]. The structure of GO has been investigated for decades, but it is substantially still unknown [20, 21, 58], and this makes GO not the ideal building block for further reactions. It was reported [59] that hydroxyl and epoxide groups are on the surface of basal planes and carbonyl and carboxyl groups are on the edges. Moreover, it is widely acknowledged that oxidation leads to extensive disruption of sp^2 hybridization of graphene layers, that is, graphene properties are drastically damaged and GO loses the benefits of a graphitic structure.

This brief sum up allows to comment that important research efforts are required in order to achieve the objective of preparing graphene and few-layer graphene (optionally containing functional groups) preserving the ideal graphene structure and through a simple, eco-friendly, economically viable and scalable method.

3. Serinol derivative for graphene functionalization

3.1. Serinol derivative: 2-(2,5-dimethyl-1H-pyrrol-1-yl)-1,3-propanediol

To pursue the (i)–(iii) objectives reported in Introduction, a serinol derivative was used: 2-(2,5-dimethyl-1H-pyrrol-1-yl)-1,3-propanediol, in the text referred to as serinol pyrrole (SP). Chemical structure of serinol pyrrole is shown in **Figure 1**.

In this paragraph, synthesis of serinol pyrrole and motivation for using such a molecule in combination with a high surface area nanosized graphite (HSAG) is discussed.

Serinol is 2-amino-1,3-propane diol that can be directly obtained from renewable sources [60] and is produced at the industrial scale from glycerol. Glycerol is a non-toxic and biodegradable raw material, cheap and easily available as it is the main co-product of biodiesel production.

http://dx.doi.org/10.5772/67630

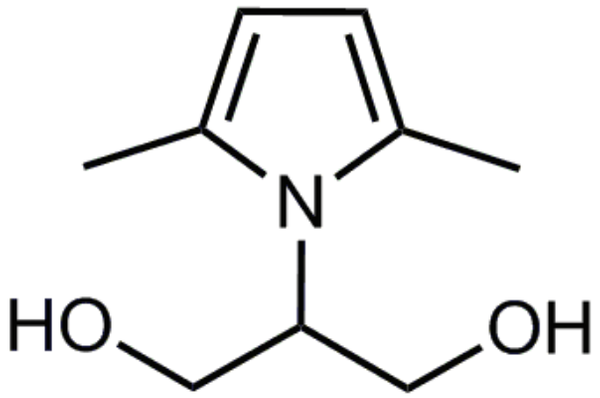


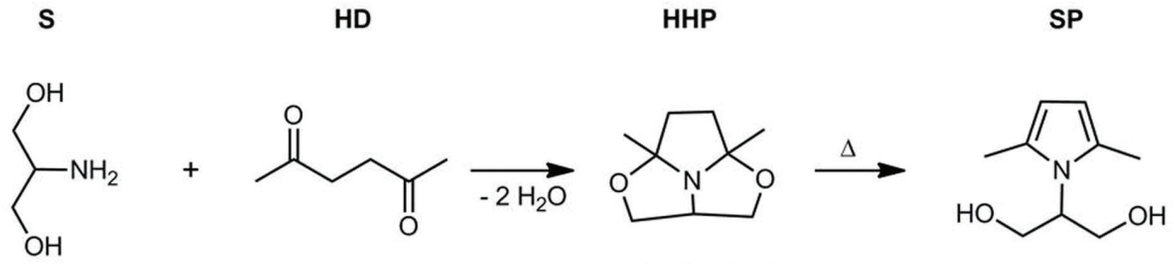
Figure 1. 2-(2,5-dimethyl-1*H*-pyrrol-1-yl)-1,3-propanediol (serinol pyrrole, SP).

Glycerol can be thus considered as a waste of an important industrial process. To use and to give added value to such a waste is particularly meaningful, as glycerol can be the building block for a C3 platform alternative to the oil-based one. It is well known that large research efforts are made nowadays to replace oil with biomass as the source for preparing chemicals and materials. First and second generation biomasses are identified. The first generation includes biomass that has impact on the food chain. For example, first-generation bioethanol is produced from sucrose, oligosaccharides and starch, whereas lignocellulose materials are used for the second-generation bioethanol. Biodiesel was produced from oil crops, whereas nowadays it is increasingly obtained from algae. In order to reduce the use of biomasses that could be employed for food production, the exploitation of wastes is encouraged. The European Parliament has made clear statements about the use of wastes and residues in place of original biomass: 'The recent experience of the development of certain renewable energy sources, particularly biofuels from food and feed crops such as cereals, oilseeds and sugar, has stimulated concern that new biorefinery processes must as far as possible be based on non-competing wastes and residues to minimize impacts on food availability and prices' [61]. More than 1 million tons of glycerol are produced per year, with a price well below 1 Euro/kg, and many routes are available for the selective conversion of glycerol to value-added products [62–65]. Serinol, produced via its reductive amination, presents the precious tool of chemoselectivity between amino and hydroxyl groups which allows in developing innovative synthetic strategies. Indeed, objective of our research was to exploit the chemoselectivity of serinol, transforming the amino moiety into a group suitable for interaction with sp^2 carbon allotropes and, in particular, with graphene layers.

3.2. Synthesis of serinol derivative, 2-(2,5-dimethyl-1H-pyrrol-1-yl)-1,3-propanediol

3.2.1. Neat synthesis

As it is shown in **Scheme 1**, Paal-Knorr reaction [66, 67] was carried out between 2-amino-1,3-propane diol (serinol, S) and 2,5-hexanedione (HD), transforming the amino group into a pyrrole ring and thus giving rise to 2-(2,5-dimethyl-1H-pyrrol-1-yl)-1,3-propanediol (SP) [68–71].



Scheme 1. Neat reaction between serinol and 2,5-hexanedione for preparing serinol pyrrole. S and HD in equimolar amount.

It is definitely worth observing that the reaction that leads to SP is characterized by very high atom economy, 82.5%, with H_2O as the only by-product. Neat reaction was carried out, in the absence of solvents and catalysts [68], with temperatures ranging from 130 to 180°C and reaction times ranging from 30 to 120 min. In Section 8, an example characterized by very high reaction yield to SP is reported: 96%. In consideration of this yield and of the atom economy, the atom efficiency is 85%.

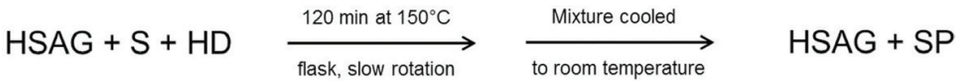
Scheme 1 reveals a two-step synthesis. The first step is the reaction between equimolar amounts of S and HD and leads to the preparation of a tricyclic compound: 4a,6a-dimethyl-hexahydro-1,4-dioxa-6b-azacyclopenta[cd]pentalene (HHP). The reaction was performed at room temperature, with almost complete conversion and selectivity, the only by-product being water (as mentioned above). In the second step of the reaction, the tricyclic compound was then isomerized to the aromatic SP, with high conversion and selectivity, by simply increasing the reaction temperature. Indeed, Nuclear Magnetic Resonance (NMR) spectra of the products of reaction steps 1 and 2 did not reveal the presence of any chemical compounds other than HHP and SP, respectively. The Paal-Knorr reaction between S and HD had been already reported [72]. Reagents were refluxed in toluene in the presence of acidic substances such as glacial acetic acid (in large amount) and *p*-toluenesulfonic acid (in catalytic amount). The product mixture contained SP in low amount (yield was about 13% mol), the tricyclic compound (HHP) and polymeric materials, whose relative amount was enhanced by acids. The neat two-step synthesis described here surprisingly led to SP with high atom efficiency. As published by some of the authors [69], this result could be ascribed, at least in part, to absence of acids and mild reaction conditions. Such experimental frame favoured, in the first reaction step, hemiaminal formation and polycyclization, preventing aromatization to SP and formation of polymeric species. Temperature increase allowed then the establishment of the thermodynamic control of the reaction.

3.2.2. Synthesis on high surface area nanographite (HSAG)

Synthesis of serinol pyrrole was as well performed on high surface area nanosized graphite, HSAG. Characteristics of HSAG are discussed in Section 4.1. The simple reaction process is shown in **Scheme 2**.

Details are in Section 8. Nuclear Magnetic Resonance (NMR) analysis of the solution of the reaction product in D_2O revealed the presence of serinol pyrrole only. This result indicates that the reaction between S and HD occurs with high yields also by supporting the ingredients on a graphitic substrate.

http://dx.doi.org/10.5772/67630



Scheme 2. Reaction between serinol (S) and 2,5-hexanedione (HD) on high surface area graphite (HSAG), for the selective preparation of serinol pyrrole (SP). S and HD are in equimolar amount.

3.3. Why to use serinol pyrrole for the functionalization of graphene layers?

SP is a serinol derivative, hence it comes from a molecule that is naturally occurring whether it comes from natural sources or from a waste such as glycerol. In the light of that, SP can be considered as a bio-sourced molecule. Its preparation appears to have also another good feature in view of a sustainable process, that is, the high atom efficiency.

By observing the chemical structure of serinol pyrrole in **Figure 1**, it can be commented that SP is a *Janus* molecule [70], that is, a molecule with two faces. Such a definition, that comes from the portray of a Roman god, was first used to indicate micro- and nanoparticles with at least two physically or chemically different surfaces [73, 74] and, subsequently, to describe molecules with two moieties (one hydrophobic and one hydrophilic) such as colloids [75] and block copolymers [76]. A *Janus* molecule is known to have a dual reactivity.

What are the two moieties in SP? One is represented by the pyrrole ring. The Paal-Knorr reaction changes the hybridization of the sp^3 nitrogen atom of the amino group and leads to the formation of sp^2 atoms in the aromatic pyrrole ring, which could give rise to π-π stacking with aromatic compounds such as graphene layers and hence to a stable interaction; moreover, the pyrrole ring could interact with lipophilic substances. Conversely, the moiety that contains hydroxy groups is hydrophilic and can promote the interaction with polar environments. Moreover, hydroxy groups can be reactive functional groups for the preparation of step growth polymers [70, 72].

Thanks to its hydrophilic moiety, SP could then promote the dispersion of graphitic aggregates in polar solvents, such as water. Exfoliation of such aggregates into few or single graphene layers could be thus promoted. As mentioned in the introduction, dilution in appropriate solvents is a method for the preparation of graphene and few-layer graphene. However, in most cases, organic (mainly aromatic) substances have to be used [22]. The structure of the graphitic substrate is expected to remain substantially unaltered by the interaction with SP: this would lead to introduce functional groups with heteroatoms such as oxygen and nitrogen on graphene layers that would maintain their pristine structure. It is evident that the success of such a design essentially depends on the strength of the interaction between SP and the graphene layers and also on the amount of SP which should be used. Moreover, the choice of the graphitic substrate for the preparation of adducts with SP appears to be of great importance.

4. Adducts of graphene layers with serinol pyrrole

In this paragraph, characteristics of HSAG (selected as the graphitic substrate) preparation and characterization of HSAG-SP adducts are discussed.

4.1. Graphitic substrate: high surface area nanosized graphite

High surface area nanosized graphite was selected for the preparation of adducts with SP. Characterization of HSAG has been already reported [57, 70, 77]. Some relevant data are shown in **Table 1**, in comparison with those of other sp^2 carbon allotropes: multiwalled carbon nanotubes (CNT) and a furnace carbon black, CBN326.

HSAG has a high surface area and is able to establish extended interactions with a polymer matrix, as shown by the diisobutyl phthalate (DBP) absorption number. By comparing HSAG and CNT data in **Table 1**, a correlation cannot be seen between surface area and DBP absorption number. As commented in previous publications [77], this finding could be explained considering that graphene layers in HSAG are stacked in crystalline domains: layers are more accessible to small nitrogen molecules used in Brunauer Emmet Teller (BET) analysis than to bulky phthalates. However, the peak shape analysis of wide angle X-ray diffraction (WAXD) pattern (shown in **Figure 2**, with the peak assignment), performed by applying the Scherrer equation to (002) reflection [56], revealed quite a low number of graphene layers stacked in a crystalline domain (about 35). Moreover, the analysis of (100) and (110) reflections, typical of the crystalline order inside the layer, allowed to estimate the shape anisotropy, defined as the ratio between the crystallites dimensions in directions parallel and orthogonal to structural layers [56]. HSAG was found to have the largest shape anisotropy, when compared with CBN326, expanded graphites and coke and calcinated petroleum cokes. (Transmission electron microscopy (TEM) analyses revealed that HSAG layers had an average size of about 300 nm [70].

Characterization of HSAG was also performed via Raman spectroscopy [70], a crucial technique for the study of carbonaceous materials [79–83]. Raman spectrum of HSAG is reported in **Figure 2** below in the text. In the Raman spectrum, two lines, named D and G, reveal the presence of graphitic sp^2-phase: they are located at 1350 cm^{-1} and 1590 cm^{-1}, respectively. Bulk crystalline graphite (graphene) gives rise to G peak, whereas the D peak occurs in the presence of either structural defects or confinement (e.g. by edges) of the graphitic layers [78, 79, 82–84]. Carbon atoms with different hybridization and grafted functional groups are indeed structural defects. Graphene layers have finite dimensions and irregular boundaries whose relative importance depends on the size of the layer. These boundaries contribute to

Carbon allotrope	Surface area[a] (m^2/g)	DBP absorption number (mL/100 g)[b]	Number of stacked layers[c]
HSAG	330	162	35
CNT[d]	200	316	10
CB N326[e]	77	85	5

[a]From BET measurements (see Ref. [78]).

[b]mL of absorbed DBP/100 g of CB (see Ref. [78]).

[c]Estimated from WAXD pattern (see Ref. [56]).

[d]Baytubes C150 P from Bayer Material Science (see Ref. [78]).

[e]From Cabot.

Table 1. Surface area, DBP absorption number and number of graphene layers stacked in crystalline domain for sp^2 carbon allotropes.

http://dx.doi.org/10.5772/67630

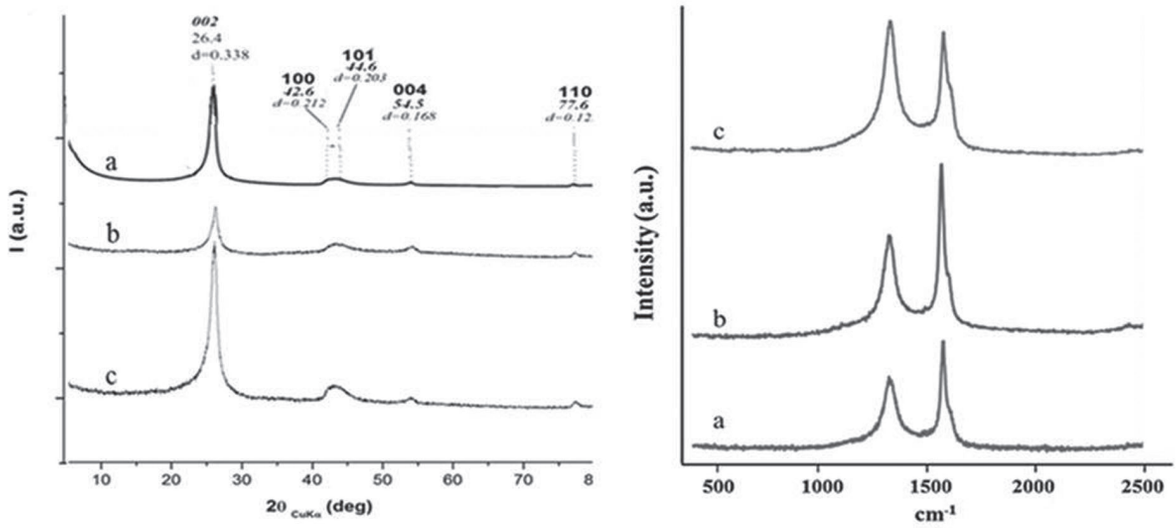


Figure 2. WAXD patterns (on the left) and Raman spectra (on the right) of HSAG (a), HSAG-SP-M (b) and HSAG-SP-T (c).

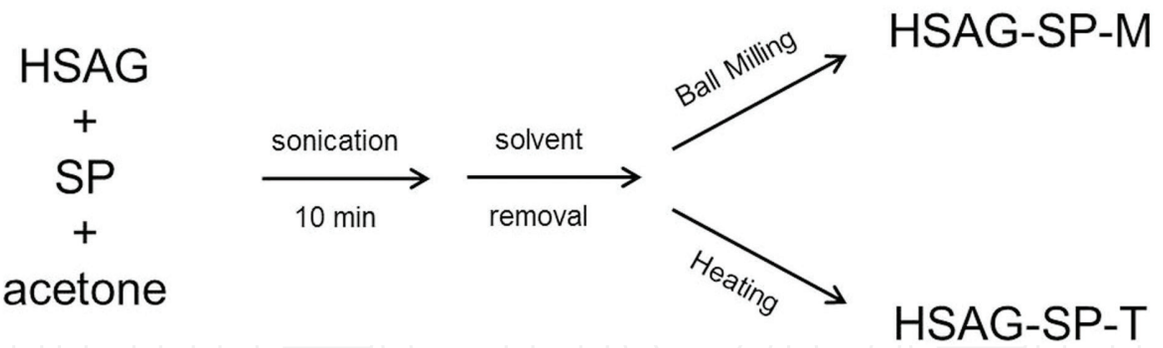
the D band. In the Raman spectrum of HSAG in **Figure 2**, both D and G bands are present, with similar intensities. To justify the intensity of the D band, some of the authors reported an interpretation [70] based on the existence of a confined crown region close to the edge, affected by confinement effects and electronically perturbed. This interpretation takes into account the small size of the HSAG graphitic layers and the obtainment of HSAG through ball milling. It was demonstrated [85] that the intensity of the D band increases in a graphitic sample by reducing the size of the layers by progressive ball milling.

HSAG appears thus an ideal substrate for the preparation of adducts with SP, thanks to the following features: high surface area, low number of stacked layers, high crystalline order inside the layers and remarkable presence of edges, that could favour interactions or even reactions with a suitable molecule.

4.2. Adducts of SP with HSAG: preparation and characterization

Adducts were prepared as illustrated in **Scheme 3**. In a nutshell, HSAG and SP were mixed in acetone, the mixture was sonicated for few minutes, solvent was removed and either mechanical or thermal energy was given to the solid HSAG-SP mixture, via ball milling or simply heating. The following adducts were prepared: HSAG-SP-M from mechanical treatment and HSAG-SP-T from thermal treatment. Typical examples of the preparation of mechanical and thermal adducts are in Section 8.

The strength of interaction between HSAG and SP was investigated. HSAG-SP adducts, upon extraction (see Section 8) were weighed and analysed through thermogravimetric analysis (TGA). As reported in a previous publication [70], the amount of SP in the adduct was estimated on the basis of the mass loss in the temperature range from 150 to 500°C. Data are collected in **Table 2**. The SP: HSAG ratio was estimated as molar ratio (the moles of HSAG are the moles of benzene rings), while the yield of functionalization was calculated by applying the following equation:



Scheme 3. Block diagram for the preparation of HSAG-SP adducts, by using either mechanical or thermal energy (for details, see Section 8).

Method	SP/HSAG molar ratio	Yield (%)
Mechanical	0.100	97.3
Thermal	0.100	91.2[b]
Thermal	0.050	79.9
Thermal	0.010	63.6
Thermal	0.005	59.5

[a]Evaluated from TGA, with the equation reported in the text.
[b]Variation coefficient, calculated for a population of 10 samples, was 1.7%.

Table 2. Preparation of HSAG-SP adducts: yield of functionalization[a].

$$\text{Yield} = \frac{\text{SP in (HSAG SP adduct)}_{\text{after the extraction}}}{\text{SP in (HSAG SP adduct)}_{\text{before the reaction}}} \times 100 \quad (1)$$

Very high yield of functionalization (larger than 90%) was achieved, both through mechanical and thermal treatments. In particular, thermal treatment with 0.1 as the SP:HSAG molar ratio gave a yield of 99%. This indicates that SP is able to establish strong interactions with HSAG. It is worth noting that the yield of functionalization decreased with the starting SP:HSAG molar ratio.

WAXD and Raman analyses were used to study the organization at the solid state of HSAG-SP adducts (details are in Ref. [71]). X-ray diffraction patterns and Raman spectra of HSAG (a), HSAG-SP-M (b) and HSAG-SP-T (c) are shown in **Figure 2**.

As regards WAXD patterns, in HSAG-SP-M and HSAG-SP-T, (002) reflection remains at the same 2θ value as in pristine HSAG, indicating that SP was not intercalated in the graphitic interlayer space. The number of layers stacked in a crystalline domain, calculated by applying the Scherrer equation to (002) reflection, as explained above, was found to decrease from HSAG (35) to HSAG-SP-T (29) to HSAG-SP-M (24). Peak shape analysis was as well performed on (100) and (110) reflections, analysing pristine HSAG and the adducts: the correlation length was found in a range from 26.5 to 28 nm. Hence, the in-plane order of HSAG was not substantially altered by the reaction with SP, even via ball milling.

http://dx.doi.org/10.5772/67630

Considering Raman characterization, D band is present in the spectrum of pristine HSAG and its relative intensity with respect to G band does not substantially change in HSAG-SP-T, after the thermal treatment. This finding suggests that the treatment with SP does not appreciably modify the structure of HSAG. On the contrary, the intensity of D band increases in HSAG-SP-M, after the mechanical treatment. In the light of what observed from WAXD analysis, the increase of disorder in the milled sample could be attributed to electronic perturbation of the confined crown region close to the edge, in line with what reported in the literature [85] about the effect of milling on graphitic samples. Different types of disorder can occur at the very edges: grafting of molecules and loss of sp^2 hybridization are among them.

The chemical nature of HSAG-SP adduct was investigated by means of FTIR analysis (experimental details are in reference [71]). The IR spectra of HSAG, HSAG-SP-T, HSAG-SP-M and SP, in the region 4000–700 cm^{-1} are reported in **Figure 3**.

The spectrum of HSAG (a) is characterized by the peak near 1590 cm^{-1} which can be assigned to the absorption of E_{1u} IR active mode of collective C=C stretching vibration of graphite/graphene materials. The increasing background towards high wavenumbers is due to diffusion/reflection phenomena of the IR beam passing through HSAG microparticles.

In the SP spectrum (d), the broad band at 3370 cm^{-1} can be reasonably attributed to hydrogen-bonded OH groups. The pyrrole ring is evidenced by the collective vibration mode of C=C/C-C stretching, located at about: 1530, 1395, 1490 and 802 cm^{-1}. Such bands can be taken as fingerprint of SP.

Spectra of extracted HSAG-SP-T and HSAG-SP-M adducts (**Figure 3b** and **c**) show bands that cannot be attributed to HSAG. Such bands are located as follows: at about 2900 cm^{-1}, in the region of sp^3 C-H stretching; at 1590 and 1470 cm^{-1}, in the region of C-C stretching of aromatic rings; at 1383 cm^{-1}, in the region of vibrations of diols and at 802 cm^{-1}, where vibration of the alkenyl groups absorbs. C-H stretching can be due to methyl groups of the pyrrole ring and to methylenes of the serinol moiety. Diols come from serinol as well. Aromatic C-C stretching is due to the presence of pyrrole ring. Moreover, in both the adducts' spectra, there are bands that are not present in either HSAG or SP spectra. Such bands are located at 1742 and 1662 cm^{-1}. Absorbances in this region are usually due to the presence of carbonyl groups. In particular, these new bands can be assigned to an aldehydic group. As reported in Section 8, the preparation of adducts is performed at high temperatures and in the presence of air. Oxidation process of the pyrrole ring could be thus hypothesized. Moreover, the efficient synthesis of graphene sheets using pyrrole as a reducing agent has been recently reported [86]: pyrrole oxidation was obtained by mixing graphene oxide with pyrrole at 95°C for 12 h.

It is worth observing that the relative intensity of the peak at 802 cm^{-1} decreases in the spectra of the adducts, in particular in the spectrum of HSAG-SP-M adduct. This peak is due to the C=C stretching of the pyrrole ring and such a reduction might lead to hypothesize that C=C bonds are involved in a chemical reaction. Working hypothesis for such a process could be the Diels-Alder reaction with the graphitic substrate. It is known that graphite is able to react with dienes and dienophiles through Diels-Alder reaction [27]. The presence of electron

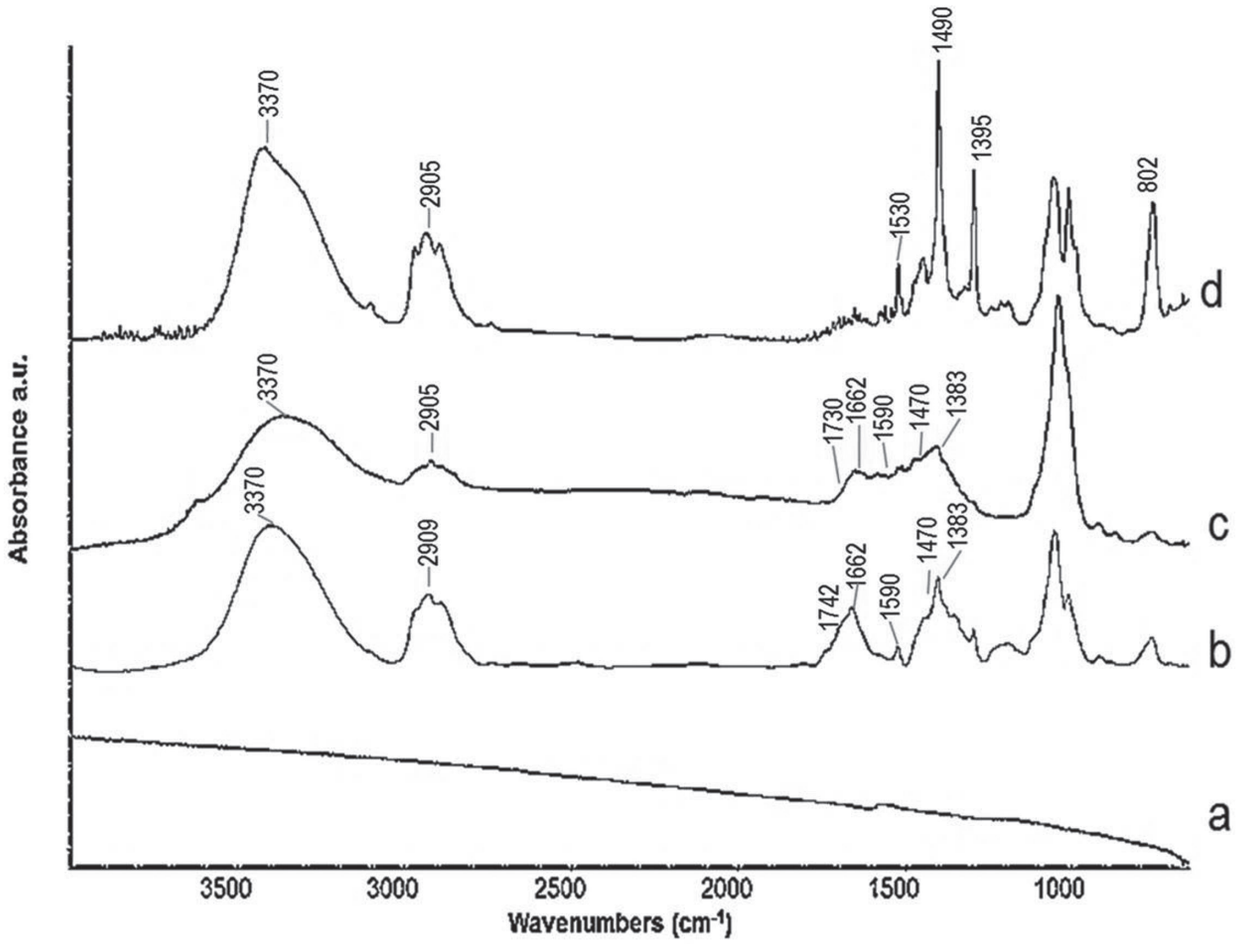


Figure 3. FTIR spectra of HSAG (a), HSAG-SP-T adduct (b), HSAG-SP-M adduct, (c) and SP (d).

withdrawing groups in alpha position with respect to the C=C bond of the pyrrole ring, as it could occur if the methyl group was oxidized to aldehyde, would favour the cycloaddition reaction.

The mechanical adduct HSAG-SP-M, with 13% by mass of SP (determined from TGA), was characterized by means of high-resolution transmission electron microscopy (HRTEM). As it has been reported [71], stable water suspensions (1 mg/mL) were prepared and samples were isolated from supernatant suspensions, after centrifugation for 10 min at 2000 rpm and for 5 and 60 min at 9000 rpm. HRTEM micrographs at lower and higher magnifications are shown in **Figure 4**.

Micrograph in **Figure 4a** reveals that the lateral size of HSAG-SP-M adduct is of few hundreds nanometers, that means of the same order of magnitude of pristine HSAG. Two comments can be made: the milling step does not appreciably affect the structure of the graphitic layers and SP promotes the dispersion in water of graphene layers with pretty large lateral size. Stacks of graphene layers (indicated in the boxes), disposed perpendicularly to the beam, are in **Figure 4b** and **c**. These figures show the most abundant stacks in populations that

contained little larger of lower number of layers. In **Figure 4b**, stacks isolated after centrifugation for 10 min at 2000 rpm are of about 3.5–4.2 nm: they are made by about 10–12 stacked graphene layers. Stack in **Figure 4c**, isolated after centrifugation for 5 min at 9000 rpm, is of about 2.8 nm and is made by about eight graphene layers.

Stacks of graphene layers can be fractionated by means of centrifugation; such fractionation appears to be prevailingly due to the number of stacks, rather than to their lateral size. Thanks to the functionalization with SP, nano-stacks of HSAG can be isolated, with a number of graphene layers which depends on the adopted experimental conditions.

4.3. Adducts of SP with other graphitic substrates

Other synthetic graphites were used for preparing adducts with SP. Their main characteristics are shown in **Table 4** in Section 8. Adducts were prepared by giving thermal energy to the graphite / SP mixture and functionalization yield was estimated by means of TGA. Values are shown in **Table 3**.

These findings indicate that the formation of graphite-SP adducts is not due to the serendipitous combination of SP with HSAG, but to the affinity and/or reactivity of the pyrrole compound with the graphitic substrate. More in particular, it is worth commenting that, in spite of the different surface area, by using 0.1 as the molar ratio between SP and the graphitic substrate, essentially the same functionalization yield was obtained.

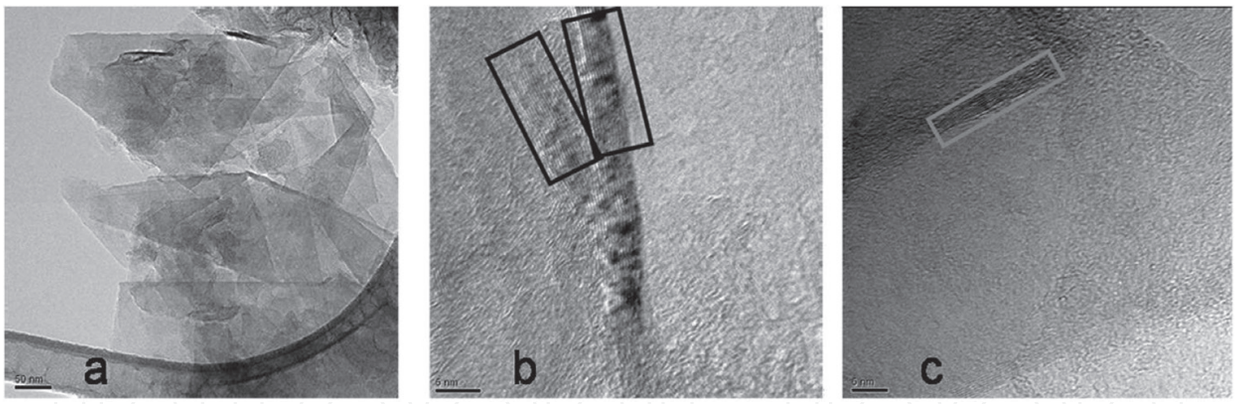


Figure 4. Micrographs of HSAG-SP-M adduct isolated from supernatant solutions, after centrifugation for 10 min at 2000 rpm (a, b) and 5 min at 9000 rpm (c). Micrographs are low magnification bright field TEM, target: 50 nm (a) and HRTEM image, target: 5 nm (b, c).

Type of graphite[a]	Nano 24	HSAG	Timrex SFG6	3807
Functionalization yield (%)	91	99	92	95

[a]Characteristics are collected in **Table 4** in Section 8.

Table 3. Graphite-SP thermal adducts: functionalization yield.

Code	Grade	C (%)	Ash (%)	Moisture (%)	Surface area (m^2/g)	Density (g/cm^3)
8427[a]	HSAG	99.8	n. a.	n. a.	330.3	n. a.
Nano 24[a]	HSAG	99.7	0.33	1.93	353.2	n. a.
3807[a]	Surface-enhanced flake graphite	98.9	n. a.	0.36	17.2	2.26
Timrex SFG6[b]	Expanded graphite	99.0	0.07	0.10	17.0	0.07

[a]Supplier: Asbury Carbon.
[b]Supplier: Imerys.

Table 4. Synthetic graphites used for the preparation of adducts with serinol pyrrole.

4.4. Adducts of SP with HSAG: what are they?

Results discussed in previous paragraphs allow commenting as follows. Serinol pyrrole and a graphitic substrate can establish a strong interaction and form very stable adducts. The functionalization of the graphitic substrate with SP leaves the bulk structure of graphene layers substantially unaltered.

The origin of such strength and stability could be attributed to the π-π interaction of the aromatic moieties, the pyrrole ring in SP and the C6 rings in the graphene layers. However, experimental indications suggest the possibility that SP is able to give rise to a chemical reaction with the aromatic layers of the substrate, more exactly to a cycloaddition reaction. More experimental data would be required to support this hypothesis. At present, rather than stretching too far intriguing inferences, it is worth examining applications that HSAG-SP adducts allow to pursue.

5. Adducts of SP and SP-based polymers with CB and CNT

This chapter is focused on the functionalization of graphene layers with a serinol derivative containing a pyrrole ring. In Section 4.3, it has been reported that the formation of stable graphite-SP adducts does not occur only by using a high-surface area nanosized graphite, such as HSAG:SP, but is indeed able to interact/react with different types of graphites.

Objective of the present paragraph is to demonstrate that SP is able to interact also with sp^2 carbon allotropes other than graphites. Adducts were formed by SP with carbon allotropes such as carbon black (CB N326) [87, 88] and multiwalled carbon nanotubes. Moreover, adducts with CNT were formed by polyurethane [69, 89] and polyethers [71, 89] oligomers containing SP as a comonomer.

CB-SP adduct [88] was prepared by using thermal energy, in the absence of solvents or catalysts, as described in Section 8. IR spectrum of the adduct, upon extraction, revealed the presence of peaks characteristic of SP. Water suspensions of CB-SP adducts were prepared and were first sonicated for 10 min and then centrifuged at 2000 rpm for 5 min. UV-Vis measurements were taken after each step of the procedure and related spectra are shown in **Figure 5a**.

http://dx.doi.org/10.5772/67630

UV-Vis absorption remained substantially the same after centrifugation. Stability of CB-SP and CB water suspensions were compared after centrifugation: suspensions are in the vials shown in **Figure 5b**. These results indicate that the treatment with SP confers a hydrophilic nature to CB, such as to allow the obtainment of stable water suspensions.

Polyurethanes (PU) oligomers (with molar mass up to about 11×10^3 g/mol) were prepared through the solvent-free polymerization of serinol pyrrole and 1,6-hexamethylene diisocyanate [69]. Adducts of such oligomers with multiwalled CNT were prepared. Suspensions in acetone of CNT-PU adducts (prepared by sonication, with 1 mg/mL as the concentration and 46% by mass of PU in the adduct) were stable even after centrifugation. HRTEM analysis of CNT-PU adduct revealed prevailingly disentangled CNTs, with intact skeleton, decorated by PU oligomers, tightly adhered to CNT surface. Micrograph of a CNT-PU adduct is shown in **Figure 6a**. Extraction tests were performed at room temperature, with ethyl acetate as the solvent, on adducts of CNT with PU oligomers with or without SP (in the latter case, 2,2-dimethyl-1,3-propanediol was the comonomer): mass loss was about 1 and 23% for the respective adducts. It is well known [90] that polyurethanes are very effective CNT modifiers, because they are able to establish very stable interaction, thanks to the π-π interaction between the carbonyl groups and the aromatic rings. It is thus worth mentioning that SP is able to enhance such interaction, revealing a sort of synergistic effect between different π systems.

Polyether (PE) oligomers (molar mass up to about 2600 g/mol) were prepared from the reaction of serinol pyrrole with 1,6-dibromo-hexane and their adducts with CNT were prepared by sonication (in acetone) [71]. Suspensions (1 mg/mL) were stable over months, even after centrifugation. HRTEM analysis revealed prevailingly disentangled CNTs, with intact skeleton, with PE oligomers wrapped on the CNT surface. Micrograph of a CNT-PE adduct is shown in **Figure 6b**. Extraction tests at room temperature with ethyl acetate were performed on CNT adducts with PE oligomers with or without SP as comonomer. Mass loss was thus about 24% for the adducts with SP based PE and 98% for the ones with a pluronic surfactant without SP.

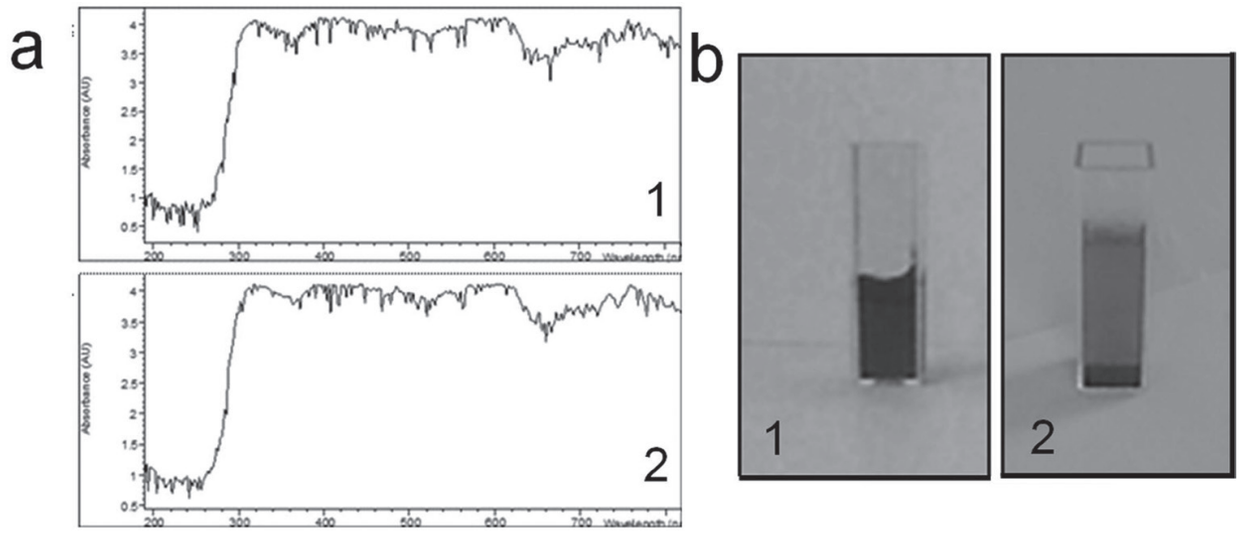


Figure 5. (a) UV-Vis spectra of water suspensions of CB-SP adduct: after sonication (1) and after centrifugation (2) and (b) water suspensions of CB-SP (1) and of CB (2), after centrifugation.

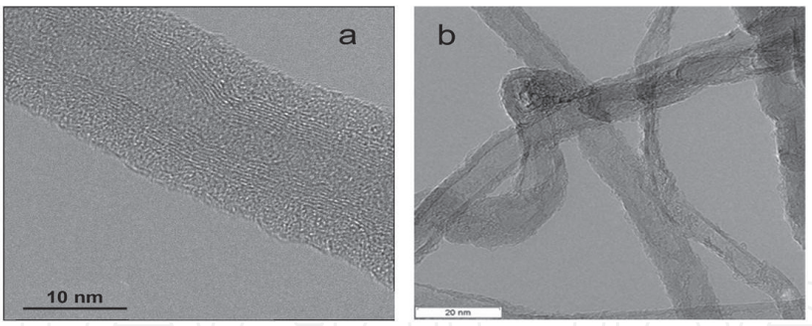


Figure 6. HRTEM micrographs of CNT-PU adduct (a), PE-CNT adduct (b). PU and PE contain serinol pyrrole as comonomer.

6. Applications of HSAG-SP adducts

As described in Section 4, HSAG and SP form stable adducts, since the aromatic moiety of the molecule is able to effectively interact with the condensed benzene rings of the graphene layers. Moreover, the hydroxy groups brought by SP promote the affinity of the adduct for polar environments. First objective was thus to prepare stable dispersions of HSAG-SP adducts in polar liquids, such as water.

6.1. Dispersions of HSAG-SP adducts in water

Water suspensions were prepared as described in Section 8, with HSAG and HSAG-SP-M adducts, with concentrations ranging from 0.1 to 30 g/L. In brief, the solid powder was suspended in water and ball milled (300 rpm, 2 hours). HSAG was observed to settle down, whereas stable suspensions were obtained with the adducts. Vials containing HSAG-SP water suspensions, with concentrations ranging from 0.10 to 10 g/L, are shown in **Figure 7**.

HSAG-SP suspensions were observed to follow the Lambert-Beer law, as it can be seen in the graph in **Figure 8a**. The UV-Vis spectra in **Figure 8b** confirm the stability of adducts' suspensions: high absorbance was recorded also upon centrifugation. It has been reported in Section 4.2 that fractionation of HSAG-SP adducts was obtained only after prolonged centrifugation, at least at 2000 rpm.

Suspensions with high HSAG-SP concentrations were prepared, up to 200 g/L. Suspensions with 10, 30 and 200 g/L concentrations are shown in **Figure 9**. Stability of the latter suspension was obtained by simply adding a small amount (1% w/w) of carboxymethylcellulose. Viscosity was observed to increase slightly, and the suspension was stable for more than a week.

6.2. Antistatic coating layers from HSAG-SP water suspensions

Water suspensions of HSAG-SP adducts are suitable for the preparation of coating layers with antistatic properties. The suspension at 200 g/L was indeed used to prepare coating layers on

http://dx.doi.org/10.5772/67630

paper, with the help of a resin to ensure the obtainment of a continuous layer and good grip with the substrate. Ratio between the adduct and the resin ranged from 90/10 to 95/5. As it is shown in **Figure 9d**, the 90/10 layer was characterized by high homogeneity. Resistivity ranged from about 2 to about 4 kOhm/sq.

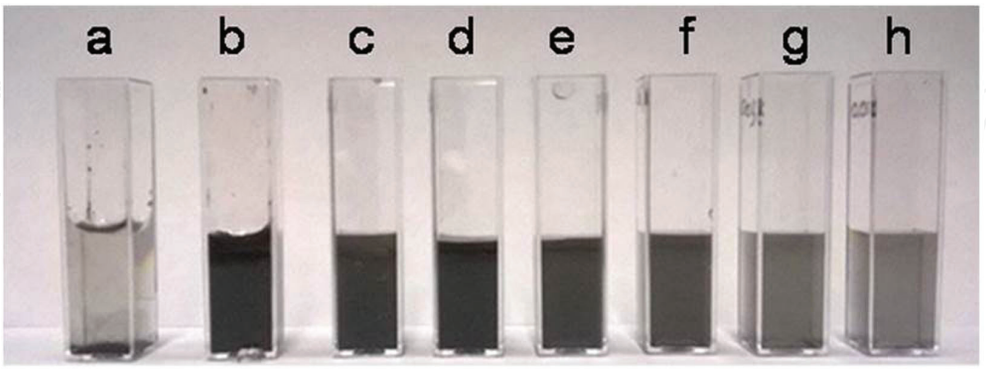


Figure 7. Water suspensions of HSAG (a) and HSAG-SP (b–h), with the following concentrations (g/L): 10 (b), 5.0 (c), 2.5 (d), 1.0 (e), 0.50 (f), 0.25 (g) and 0.10 (h).

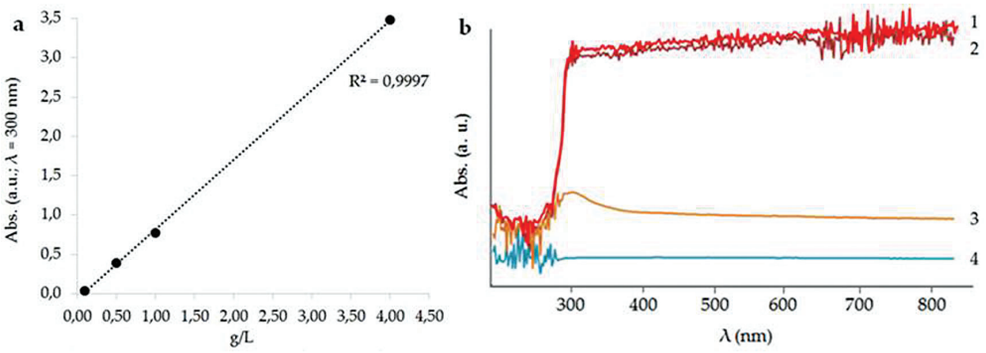


Figure 8. Dependence of UV-Vis absorbance of HSAG-SP-M (1 mg/mL) water suspensions on concentration (g/L) (a) and on storage, sonication and centrifugation (9000 rpm) (b): after sonication (1), after storage at rest for 1 week (2), after centrifugation at 9000 rpm for 10 min (3). UV-Vis spectrum of HSAG water suspension after centrifugation at 9000 rpm for 10 min as a reference (4).

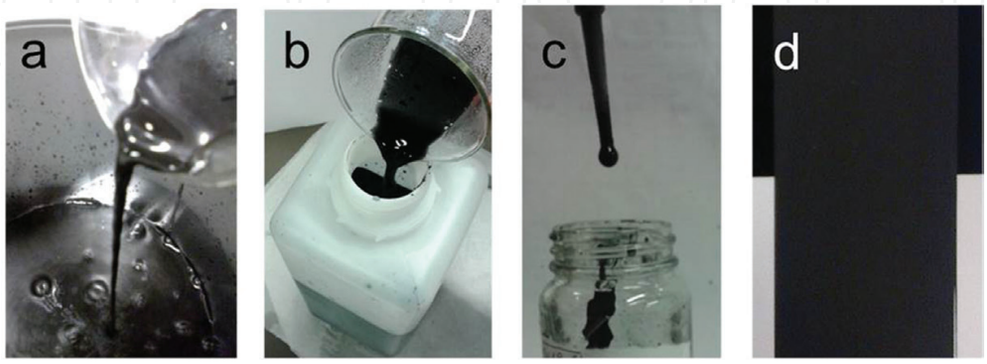


Figure 9. Aqueous suspensions of HSAG-SP with the following concentrations: (a) 10 g/L, (b) 30 g/L and (c) 200 g/L. Coating layer of HSAG-SP adduct on paper substrate (see text) (d).

6.3. Nanocomposites with few-layer graphene in natural rubber as the matrix

Poly(1,4-cis-isoprene) from *hevea brasiliensis* is known as natural rubber (NR) and is the most important rubber, accounting for about 60% of the global rubber market, with a worldwide production of more than 12 million tons per year [91, 92]. It is well known that NR comes from the tree in a latex. The chance of preparing stable water dispersions of HSAG was exploited to obtain homogeneous dispersions of HSAG in NR matrix. Details are in Section 8. Procedure is summarized in **Scheme 4**.

In **Figure 10**, TEM micrograph at high magnification of the nanocomposite formed by NR and HSAG-SP is shown. Stacks of only a few graphene layers and also isolated graphene layers are visible.



Scheme 4. Procedure for the preparation of NR/HSAG-SP nanocomposite from NR latex.

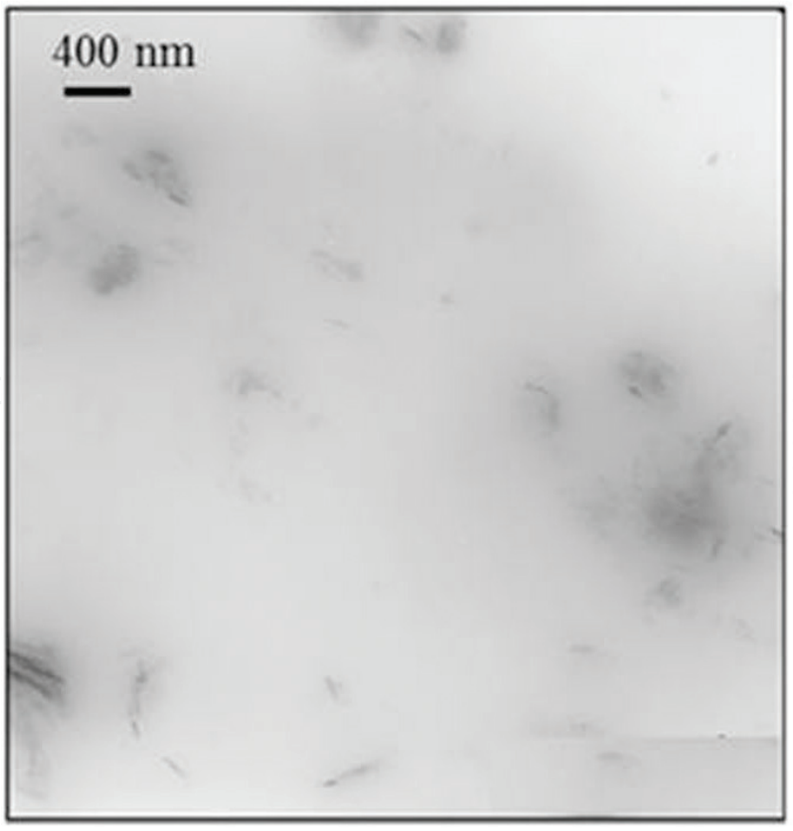


Figure 10. TEM micrograph of NR/HSAG-SP nanocomposite.

Latex pre-mixing of nanographite has been indicated [93–95] as the best procedure to obtain highly homogeneous distribution of nanoparticles. Graphene layers are placed around NR globules and form interconnected networks. Low electrical percolation threshold is achieved with low nanographite contents. It is well known that rubber composites are prepared through melt blending that should not only make the latex mixing step redundant, but should also destroy the interconnected network. However, even after melt blending, more homogeneous nanographite dispersion is documented in nanocomposites obtained first via latex blending. In the mentioned references, graphitic layers come from chemically reduced graphite oxide [93], thermally exfoliated graphite oxide [94] and expanded graphite [95] that means from graphites that require relevant treatments.

6.4. Dispersions of HSAG-SP adducts in polyols

Dispersions of HSAG-SP were as well prepared in polyols, as described in Section 8. The goal was to obtain highly homogeneous stable dispersion of graphene layers in a polyol, which means in a precursor of polyurethanes (PUs). PUs are important polymers that account for about 5% of worldwide polymer production and experience an increasing market penetration. Main drawback is their insufficient fire behaviour. Graphite layers are known to impart intumescent properties to polymer materials. However, due to their poor affinity for the polymeric matrices, they can be hardly dispersed in polyols and have been observed to settle down in short times. In the research reported here, three types of graphites (see **Table 4** in Section 8) were used and stable dispersions were obtained, with concentrations from 2 to 10, as mass%. For example, the suspension with 2% by mass as HSAG-SP concentration (SP content: 23.5% by mass) was analysed via UV-Vis spectrophotometry over a month period, observing stable absorption. It is worth commenting that unmodified graphites clearly settled down even after few days. Moreover, the same HSAG-SP suspension was centrifuged at 3000 rpm for 45 min. The supernatant suspension revealed the same UV absorption. In **Figure 11**, 2% by mass suspensions are shown. They were easily prepared (see in Section 8) and are suitable for large-scale productions.

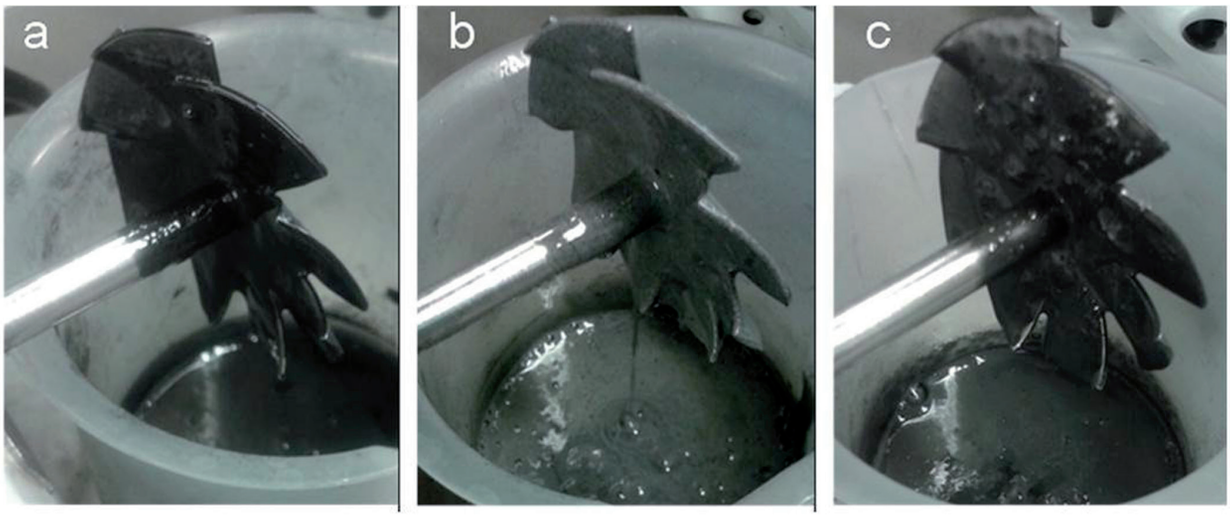


Figure 11. Suspensions in polyol of HSAG Nano 24 (a), flake graphite 3807 (b) and expanded graphite Timrex SFG6 (c).

7. Conclusions

Functionalization of graphene layers was performed with a serinol derivative containing a pyrrole ring: 2-(2,5-dimethyl-1H-pyrrol-1-yl)-1,3-propanediol, named as serinol pyrrole.

Synthesis of SP was characterized by very high atom economy and yield and thus by a high atom efficiency, close to 90%. A high surface area nanosized graphite was preferentially used as the graphitic substrate, but the reaction with SP was successful with other types of graphite and of sp^2 carbon allotropes, such as carbon black and carbon nanotubes.

Reaction was performed by simply mixing SP and the carbon allotrope and giving either mechanical or thermal energy.

SP and the graphitic substrate revealed strong interaction and formed very stable adducts. Such stability could be explained with the π-π interaction of the aromatic moieties, the pyrrole ring in SP and the C6 rings in the graphene layers. However, experimental indications seem to support the occurring of a chemical reaction between SP and the aromatic layers of the substrate, more exactly a cycloaddition reaction.

By centrifuging water suspensions of HSAG-SP adducts, stacks of few layers graphene were isolated. The procedure based on the preparation of water suspensions of HSAG-SP adducts and the subsequent centrifugation appears to be a promising, environmentally friendly method for obtaining layers of graphene.

HSAG-SP adducts allow to envisage a large variety of applications. They form very stable suspensions in water and polyols. Antistatic coating layers have been already prepared and work for the preparation of polyurethanes is in progress. Very homogeneous dispersion has been obtained for graphene layers in natural rubber matrix.

8. Experimental

8.1. Materials

Four grades of graphite have been modified and used in the course of our studies. Their features are summarized in **Table 4**.

Other reagents, described in detail in cited references, were purchased and used without further purifications.

8.2. Synthesis of 2-(2,5-dimethyl-1H-pyrrol-1-yl)-1,3-propanediol (serinol pyrrole, SP)

A mixture of hexan-2,5-dione (41.40 g; 0.36 mol) and serinol (30.00 g; 0.33 mol) was poured into a 100 mL round bottomed flask equipped with a magnetic stirrer. The mixture was then stirred, at room temperature, for 6 hours. The yield of the resulting intermediate compound 4a,6a-dimethyl-hexahydro-1,4-dioxa-6b-azacyclopenta[cd]pentalene was estimated to be 99%. Then the mixture was kept under vacuum for 2 hours and subsequently heated to 180°C

for 50 min. After distillation under reduced pressure at 130°C and 0.1 mbar, serinol pyrrole (indicated as SP from now on) was isolated as yellow oil with 96% yield [68–70].

8.3. Synthesis of SP on high surface area graphite as the carbon allotrope

A total of 0.20 g of HSAG, 0.08 g of serinol (0.922 mmol) and 0.11 g of 2,5-hexanedione (0.922 mmol) were put in a 50 mL round bottom flask, which was also equipped with a magnetic stirrer. The reaction mixture was left to stir at 150°C for 120 min, then it was cooled to room temperature. A sample of black powder was put in a test tube and suspended with deuterated water (D_2O); the so obtained heterogeneous mixture was filtered through a PTFE 0.2 μm filter. The liquid passing through the filter was analysed by Proton Nuclear Magnetic Resonance spectroscopy (^{1}H-NMR). NMR spectrum revealed signals that could be attributed only to SP.

8.4. Preparation of HSAG-SP adducts

HSAG-SP adducts were prepared by reacting HSAG and SP with the help of either mechanical (HSAG-SP-M) or thermal (HSAG-SP-T) energy.

8.4.1. HSAG-SP-M adduct

HSAG (0.05 g, 66 mmol) and acetone (15 mL) were put in sequence in a 100 mL round bottom flask. The suspension was sonicated for 15 min, using a 2 L ultrasonic bath. After this time, a solution of SP (5.87 g, 66 mmol) in acetone (15 mL) was added and the mixture was sonicated for 15 min. The solvent was then removed under reduced pressure and the graphite/SP black powder was treated using a planetary ball mill whose grinding jar was loaded with six ceramic balls (diameter = 20 mm). After 6 hours of rotation at a rate of 300 rpm, the mixture was thoroughly washed with distilled water (6 × 100 mL) on a funnel with a sintered glass filter and dried in air overnight. A total of 9.80 g of black powder was recovered [70].

8.4.2. HSAG-SP-T adduct

HSAG (5.00 g, 66 mmol), acetone (15 mL) and a solution of SP (1.12 g, 6.6 mmol) in acetone (5 mL) were put in a 100 mL round bottom flask and sonicated as described in Section 8.4.1. Then, after removing the solvent under reduced pressure, the flask was equipped with a magnetic stirrer and the mixture was heated at 130°C for 6 hours under vigorous stirring. After cooling at room temperature, the mixture was repeatedly washed with distilled water (3 × 20 mL) on a funnel with a sintered glass filter and finally dried in air overnight. A total of 5.86 g of black powder was obtained.

8.5. Extraction of HSAG-SP adducts

HSAG-SP adducts were washed using a Soxhlet extractor. In a typical procedure, 3.00 g of black powder was put inside a thimble, which was loaded into the main chamber of the Soxhlet extractor. Acetone was used as the extraction solvent and was placed in a distillation flask. The flask was heated at 70°C, and the extraction was continually performed for 12 hours.

After this time, the thimble was removed from the main chamber of the Soxhlet extractor; the powder was recovered and then dried in an oven at 70°C for some hours [70].

8.6. Preparation of water suspensions of HSAG-SP adducts, evaluation of their stability and microscopic characterization

Water suspensions of HSAG-SP adducts at different concentrations (1 mg/mL; 0.5 mg/mL; 0.3 mg/mL; 0.1 mg/mL) were prepared. Each solution was sonicated for 10 min using an ultrasonic bath (260 W) and subsequently UV-Vis absorption was measured. The solution (10 mL) of each sample was put in a Falcon™ 15 mL conical centrifuge tubes and centrifuged at: 2000 rpm for 10 min and at 9000 rpm for 10, 30, 60 and 90 min. After each centrifugation step, supernatant fluids were picked up, transferred into a cuvette and analysed. UV-Vis absorptions and DLS analysis were measured immediately after each centrifugation and after 1 week storage.

HRTEM investigations on adducts' samples, isolated from the supernatant solutions after centrifugation, were carried out with a Philips CM 200 field emission gun microscope operating at an accelerating voltage of 200 kV. Few drops of the aqueous solutions were deposited on 200 mesh lacey carbon-coated copper grid and air-dried for several hours before analysis. During acquisition of HRTEM images, the samples did not undergo structural transformation. Low-beam current densities and short acquisition times were adopted. To estimate the number of stacked graphene layers and the dimensions of the stacks visible in HRTEM micrographs, the Gatan Digital Micrograph software was used.

8.7. Preparation of polyol suspensions of HSAG-SP adducts

The adducts of SP with Nano 24, 3807 and Timrex SFG6 (SP: graphite = 0.1 molar ratio) were prepared following the procedure described in Section 8.4.2; they were subsequently purified by suspending them in acetone (15 mL every gram of adduct), letting the suspension stir overnight and filtering it over a funnel with a sintered glass filter. The powder was subsequently washed several times with acetone until colourless washings and dried in air overnight.

Samples at 2, 5 and 10% (w/w) concentrations of the three SP-graphite adducts in polyol (Aropol 424™, supplier Pozzi Arosio SAS) were obtained by slowly pouring the chosen grey-black dry powder into a vessel containing the viscous liquid while vigorously stirring with a laboratory rod stirrer. After 30 min, the mixture was recovered and stored in PET bottles.

8.8. Preparation of CB-SP adducts

Carbon black (1.00 g) and acetone (15 mL) were transferred to a 100 mL round bottom flask and the obtained suspension was sonicated for 15 min, using a 2 L ultrasonic bath. After this time, a solution of SP (0.24 g) in acetone (15 mL) was added. The mixture was sonicated for 15 min. After removing the solvent under reduced pressure, a black powder of SP absorbed carbon black was obtained; 0.70 g of this powder were placed in a vial equipped with a magnetic stirrer. The reaction mixture was heated at 180°C for 2 hours and then let to cool at

room temperature; the product was thoroughly washed with distilled water (3 × 100 mL) on a funnel with a sintered glass filter and finally dried in air overnight.

Author details

Maurizio Galimberti*, Vincenzina Barbera and Annalisa Sironi

*Address all correspondence to: maurizio.galimberti@polimi.it

Department of Chemistry, Materials and Chemical Engineering "G. Natta", Polytechnic University of Milan, Milan, Italy

References

[1] Novoselov K. S., Geim A. K., Morozov S. V., Jiang D., Zhang Y., Dubonos S. V., Grigorieva I. V., Firsov A. A. (2004) Electric field effect in atomically thin carbon films. Science 306: 666–669.

[2] Geim A. K., MacDonald A. H. (2007) Graphene: exploring carbon flatland. Phys. Today 60: 35–42.

[3] Geim A. K., Novoselov K. S. (2007) The rise of graphene. Nat. Mater. 6: 183–191.

[4] Zhang Y., Tan J. W., Stormer H. L., Kim P. (2005) Experimental observation of the quantum hall effect and Berry's phase in graphene. Nature 438: 201–204.

[5] Novoselov K. S., Geim A. K., Morozov S. V., Jiang D., Katsnelson M. I., Grigorieva I. V., Dubonos S. V., Firsov A. A. (2005) Two-dimensional gas of massless Dirac fermions in graphene. Nature 438 (7065): 197–200.

[6] Balandin A. A. (2011) Thermal properties of graphene and nanostructured carbon materials. Nat. Mater. 10: 569–581.

[7] Chen S., Wu Q., Mishra C., Kang J., Zhang H., Cho K., Cai W., Balandin A. A., Ruoff R. S. (2012) Thermal conductivity of isotopically modified graphene. Nat. Mater. 11: 203–207.

[8] Thostenson E. T., Li C. Y., Chou T. W. (2005) Nanocomposites in context. Comp. Sci. Technol. 65: 491–516.

[9] Stankovich S., Dikin D. A., Dommett G. H. B., Kohlhaas K. M., Zimney E. J., Stach E. A., Piner R. D., Nguyen S. T., Ruoff R. S. (2006) Graphene-based composite materials. Nature. 442: 282–286.

[10] Singh V., Joung D., Zhai L., Das S., Khondaker S. I., Seal S. (2011) Graphene based materials: past, present and future. Progr. Mater. Sci. 56: 1178–1271.

[11] Wang X., Zhi J., Mullen K. (2008) Transparent, conductive graphene electrodes for dye-sensitized solar cells. Nano Lett. 8: 323–327.

[12] Pushparaj V. L., Shaijumon M. M., Kumar A., Murugesan S., Ci L., Vajtai R., Linhardt R. J., Nalamasu O., Ajayan P. M. (2007) Flexible energy storage devices based on nanocomposite paper. Proc. Natl. Acad. Sci. USA. 104 (34): 13574–13577.

[13] Waje M. M., Wang X., Li W., Yan Y. (2005) Deposition of platinum nanoparticles on organic functionalized carbon nanotubes grown in situ on carbon paper for fuel cells. Nanotechnology 16 (7): 395–400.

[14] Yagoh H., Murayama H., Suzuki T., Tominaga Y., Shibuya N., Masuda Y. (2006) Simultaneous monitoring method of polycyclic aromatic hydrocarbons and persistent organic pollutants in the atmosphere using activated carbon fiber filter paper. Anal. Sci. 22 (4) 583–590.

[15] Zheng F., Baldwin D. L., Fifield L. S., Anheier Jr N. C., Aardahl C. L., Grate J.W. (2006) Single-walled carbon nanotube paper as a sorbent for organic vapor preconcentration. Anal. Chem. 78 (7): 2442–2446.

[16] Coleman J. N., Blau W. J., Dalton A. B., Muñoz E., Collins S., Kim B. G., Razal J., Selvidge M., Vieiro G., Baughman R. H. (2003) Improving the mechanical properties of single-walled carbon nanotube sheets by intercalation of polymeric adhesives. Appl. Phys. Lett. 82 (11): 1682–1684.

[17] Navalon S., Dhakshinamoorthy A., Alvaro M., Garcia H. (2014) Carbocatalysis by graphene-based materials. Chem. Rev. 114: 6179−6212.

[18] Chua C. K., Pumera M. (2015) Carbocatalysis: the state of "metal-free" catalysis. Chem. Eur. J. 21: 12550–12562.

[19] Dreyer D. R., Bielawski C. W. (2011) Carbocatalysis: heterogeneous carbons finding utility in synthetic chemistry. Chem. Sci. 2: 1233–1240.

[20] Hernandez Y., Pang S., Feng X., Müllen K. (2012) Graphene and Its Synthesis. Polymer Science: A Comprehensive Reference 8: 415-438, Eds. Matyjaszewski K., Möller M.; Elsevier B. V.

[21] Randviir E. P., Brownson D. A. C., Banks C. E. (2014) A decade of graphene research: production, applications and outlook. Mater. Today 17 (9): 426–432.

[22] Coleman J. N., Lotya M., O'Neill A., Bergin S. D., King P. J., Khan U., Young K., Gaucher A., De S., Smith R. J., Shvets I. V., Arora S. K., Stanton G., Kim H. Y., Lee K., Kim G. T., Duesberg G. S., Hallam T., Boland J. J., Wang J. J., Donegan J. F., Grunlan J. C., Moriarty G., Shmeliov A., Nicholls R. J., Perkins J. M., Grieveson E. M., Theuwissen K., McComb D. W., Nellist P. D., Nicolosi V. (2011) Two-dimensional nanosheets produced by liquid exfoliation of layered materials. Science 331: 568–571.

[23] Plummer J. (2015) Graphene synthesis: molten bed. Nat. Mater. 14: 1186–1186.

[24] Eigler S., Grimm S., Hof F., Hirsch A. (2013) Graphene oxide: a stable carbon framework for functionalization. J. Mater. Chem. A 1: 11559–11562.

[25] Dreyer D. R., Park S., Bielawski C. W., Ruoff R. S. (2010) The chemistry of graphene oxide. Chem. Soc. Rev. 39: 228–240.

[26] Collins W. R., Lewandowski W., Schmois E., Walish J., Swager T. M. (2011) Claisen rearrangement of graphite oxide: a route to covalently functionalized graphenes. Angew. Chem. Int. Ed. 50: 8848–8852.

[27] Sarkar S., Bekyarova E., Haddon R. C. (2012) Chemistry at the Dirac point: Diels-Alder reactivity of graphene. Acc. Chem. Res. 45 (4): 673–682.

[28] Swager T. M. (2012) Functional graphene: top-down chemistry of the π-surface. ACS Macro. Lett. 1: 3–5.

[29] Zaman I., Kuan H.-C., Meng Q., Michelmore A., Kawashima N., Pitt T., Zhang L., Gouda S., Luong L., Ma J. (2012) A facile approach to chemically modified graphene and its polymer nanocomposites. Adv. Funct. Mater. 22 (13): 2735–2743.

[30] Huang X., Qi X., Boeya F., Zhang H. (2012) Graphene-based composites. Chem. Soc. Rev. 41: 666–686.

[31] Chua C. K., Pumera M. (2013) Covalent chemistry on graphene. Chem. Soc. Rev. 42: 3222–3233.

[32] Englert J. M., Dotzer C., Yang G., Schmid M., Papp C., Gottfried J. M., Steinrück H.-P., Spiecker E., Hauke F., Hirsch A. (2011) Covalent bulk functionalization of graphene. Nat. Chem. 3: 279–286.

[33] Toth P. S., Ramasse Q. M., Velický M., Dryfe R. A. W. (2015) Functionalization of graphene at the organic/water interface. Chem. Sci. 6: 1316–1323.

[34] Brodie B. C. (1859) On the atomic weight of graphite. Philos. Trans. R. Soc. Lond. 14: 249–259.

[35] Lopez M. I., Croce A. E., Sicre J. E. (1994) Explosive decomposition of gaseous chlorine dioxide. J. Chem. Soc. Faraday Trans. 90 (22): 3391–3396.

[36] Poh H. L., Sanek F., Ambrosi A., Zhao G., Sofer Z., Pumera M. (2012) Graphenes prepared by Staudenmaier, Hofmann and Hummers methods with consequent thermal exfoliation exhibit very different electrochemical properties. Nanoscale. 4 (11): 3515–3522.

[37] Staudenmaier L. (1898) Process for the preparation of the graphitic acid. Ber. Dtsch. Chem. Ges. 31: 1481-1487.

[38] Hummers W. S., Offeman R. E. (1958) Preparation of graphitic oxide. J. Am. Chem. Soc. 80: 1339–1339.

[39] Ang P. K., Wang S., Bao Q., Thong J. T. L., Loh K. P. (2009) High-throughput synthesis of graphene by intercalation–exfoliation of graphite oxide and study of ionic screening in graphene transistor. ACS Nano 3 (11): 3587–3594.

[40] Marcano D. C., Kosynkin D. V., Berlin J. M., Sinitskii A., Sun Z., Slesarev A., Alemany L. B., Lu W., Tour J. M. (2010) Improved synthesis of graphene. ACS Nano 4 (8): 4806–4814.

[41] Chen J., Yao B., Li C., Shi G. (2013) An improved Hummers method for eco-friendly synthesis of graphene oxide. Carbon 64: 225–229.

[42] Chen J., Li Y., Huang L., Li C., Shi G. (2015) High-yield preparation of graphene oxide from small graphite flakes via an improved Hummers method with a simple purification process. Carbon 81: 826–834.

[43] Guerrero-Contreras J., Caballero-Briones F. (2015) Graphene oxide powders with different oxidation degree, prepared by synthesis variations of the Hummers method. Mater. Chem. Phys. 153: 209–220.

[44] Kovtyukhova N. I., Ollivier P. J., Martin B. R., Mallouk T. E., Chizhik S. A., Buzaneva E. V., Gorchinskiy A. D. (1999) Layer-by-layer assembly of ultrathin composite films from micron-sized graphite oxide sheets and polycations. Chem. Mater. 11 (3): 771–778.

[45] Posudievsky O. Yu., Khazieieva O. A., Koshechko V. G., Pokhodenko V. D. (2012) Preparation of graphene oxide by solvent-free mechanochemical oxidation of graphite. J. Mater. Chem. 22: 12465–12467.

[46] Galimberti M., Cipolletti V., Mauro M., Conzatti L. (2013) Nanocomposites of Poly(1,4-cis-Isoprene) with graphite oxide intercalation compounds. Macromol. Chem. Phys. 214 (17): 1931–1939.

[47] Boehm H. P., Clauss A., Fischer G. O., Hofmann U. (1962) Dünnste Kohlenstoff-Folien. Z. Naturforsch Pt. B. 17 (3): 150–153.

[48] Eda G., Fanchini G., Chhowalla M. (2008) Large-area ultrathin films of reduced graphene oxide as a transparent and flexible electronic material. Nat. Nanotechnol. 3 (5): 270–274.

[49] Gomez-Navarro C., Weitz R. T., Bittner A. M., Scolari M., Mews A., Burghard M., Kern K. (2007) Electronic transport properties of individual chemically reduced graphene oxide sheets. Nano Lett. 7 (11): 3499–3503.

[50] Stankovich S., Dikin D. A., Piner R. D., Kohlhaas K. A., Kleinhammes A., Jia Y., Wu Y., Nguyen S. T., Ruoff R. S. (2007) Synthesis of graphene-based nanosheets via chemical reduction of exfoliated graphite oxide. Carbon 45: 1558–1565.

[51] Li D., Muller M. B., Gilje S., Kaner R. B., Wallace G. G. (2008) Processable aqueous dispersions of graphene nanosheets. Nat. Nano. 3 (2):101–105.

[52] Fan X. B., Peng W., Li Y., Li X., Wang S., Zhang G., Zhang F. (2008) Deoxygenation of exfoliated graphite oxide under alkaline conditions: a green route to graphene preparation. Adv. Mater. 20 (23): 4490–4493.

[53] Abdolhosseinzadeh S., Asgharzadeh H., Kimb H. S. (2015) Fast and fully-scalable synthesis of reduced graphene oxide. Sci. Rep. 5: 10160–10166.

[54] You F., Wang D., Cao J., Li X., Dang Z.-M., Hu G.-H. (2014) In situ thermal reduction of graphene oxide in a styrene–ethylene/butylene–styrene triblock copolymer via melt blending. Polym. Int. 63: 93–99.

[55] Cote L. J., Cruz-Silva R., Huang J. (2009) Flash reduction and patterning of graphite oxide and its polymer composite. J. Am. Chem. Soc. 131: 11027–11032.

[56] Mauro M., Cipolletti V., Galimberti M., Longo P., Guerra G. (2012) Chemically reduced graphite oxide with improved shape anisotropy. J. Phys. Chem. C 116 (46): 24809–24813.

[57] Schniepp H. C., Li J.-L., McAllister M. J., Sai H., Herrera-Alonso M., Adamson D. H., Prud'homme R. K., Car R., A. Saville D. A., Aksay I. A. (2006) Functionalized single graphene sheets derived from splitting graphite oxide. J. Phys. Chem. B 110 (17): 8535–8539.

[58] He H., Klinowski J., Forster M., Lerf A. (1998) Structure of graphite oxide revisited. Chem. Phys. Lett. 287 (1–2): 53–56.

[59] Zhu Y., Murali S., Cai W., Li X., Suk J. W., Potts J. R., Ruoff R. S. (2010) Graphene and graphene oxide: synthesis, properties, and applications. Adv. Mater. 22: 3906–3924.

[60] Andreeßen B. A. S. (2011) Serinol: small molecule - big impact. AMB Express 1: 1–6.

[61] European Parliament (2013) Technology options for feeding 10 billion people. Science and Technology Options Assessment.

[62] Pagliaro M., Ciriminna R., Kimura H., Rossi M., Della Pina C. (2007) From glycerol to value added products. Angew. Chem. Int. Ed. 46: 4434–4440.

[63] Zhou C.-H., Beltramini J. N., Fana Y.-X., Lu G. Q. (2008) Chemoselective catalytic conversion of glycerol as a biorenewable source to valuable commodity chemicals. Chem. Soc. Rev. 37 (3): 527–549.

[64] Yang F., Hanna M. A., Sun R. (2012) Value-added uses for crude glycerol – a by-product of biodiesel production. Biotechnol. Biofuels 5: 13.

[65] Jérôme F., Pouilloux Y., Barrault J. (2008) Rational design of solid catalysts for the selective use of glycerol as a natural organic building block. Chem. Sus. Chem. 1 (7): 586–613.

[66] Knorr L. (1885) Effect of diethyl succinate on ammonia and primary amine bases. Chem. Ber. 18: 299.

[67] Paal C. (1885) Synthesis of thiophene and pyrrole derivatives. Chem. Ber. 18: 367.

[68] Barbera V., Citterio A., Galimberti M., Leonardi G., Sebastiano R., Shisodia S. U., Valerio A. M. (2015) Process for the synthesis of 2-(2,5-dimethyl-1h-pyrrol-1-yl)-1,3-propanediol and its substituted derivatives. WO2015189411 A1.

[69] Galimberti M., Barbera V., Citterio A., Sebastiano R., Truscello A., Valerio A. M., Conzatti L., Mendichi R. (2015) Supramolecular interactions of carbon nanotubes with biosourced polyurethanes from 2-(2,5-dimethyl-1H-pyrrol-1-yl)-1,3-propanediol. Polymer 63: 62–70.

[70] Galimberti M., Barbera V., Guerra S., Conzatti L., Castiglioni C., Brambilla L., Serafini A. (2015) Biobased janus molecule for the facile preparation of water solutions of few layer graphene sheets. RSC Adv. 5: 81142–81152.

[71] Barbera V., Musto S., Citterio A., Conzatti L., Galimberti M. (2016) Polyether from a biobased Janus molecule as surfactant for carbon nanotubes. Express Polym. Lett. 10 (7): 548–555.

[72] Broadbent H. S., Burnham W. S., Sheeley R. M., Olsen R. K. (1976) Novel heterotricyclic systems: 2,6-dioxa- and 2-oxa-6-thia-10-azatricyclo-[5.2.1.$0^{4,10}$] decanes; 2,6-dioxa-11-azatricyclo[5.3.1.$0^{4,11}$] undecane; and 9,13-dioxa-14-azatetracyclo[6.5.1.$0^{2,7}$.$0^{11,14}$]tetradeca-2,4,6-triene. J. Heterocycl. Chem. 13 (2): 337–348.

[73] Casagrande C., Fabre P., Veyssie M., Raphael E. (1989) "Janus Beads": realization and behaviour at water/oil interfaces. Europhys. Lett. 9 (3): 251–255.

[74] de Gennes P. G. (1992) Soft matter (Nobel lecture). Angew. Chem. Int. Ed. 31 (7): 842–845.

[75] Li F., Josephson D. P., Stein A. (2011) Colloidal assembly: the road from particles to colloidal molecules and crystals. Angew. Chem. Int. Ed. 50 (2): 360–388.

[76] Mori H., Müller A. H. (2003) New polymeric architectures with (meth)acrylic acid segments. Progr. Polym. Sci. 28 (10): 1403–1439.

[77] Agnelli S., Cipolletti V., Musto S., Coombs M., Conzatti L., Pandini S., Riccò T., Galimberti M. (2014) Interactive effects between carbon allotrope fillers on the mechanical reinforcement of polyisoprene based nanocomposites. Expr. Polym. Lett. 8 (6): 436–449.

[78] Reich S., Thomsen C. (2004) Raman spectroscopy of graphite. Phil. Trans. Roy. Soc. Lond. A 362 (1824): 2271–2288.

[79] Castiglioni C., Tommasini M., Zerbi G. (2004) Raman spectroscopy of polyconjugated molecules and materials: confinement effect in one and two dimensions. Phil. Trans. Roy. Soc. Lond. A 362 (1824): 2425–2459.

[80] Ferrari A. C. (2007) Raman spectroscopy of graphene and graphite: disorder, electron–phonon coupling, doping and nonadiabatic effects. Sol. State Commun. 143: 47–57.

[81] Pimenta M. A., Dresselhaus G., Dresselhaus M. S., Cancado L. G., Jorio A., Saito R. (2007) Studying disorder in graphite-based systems by Raman spectroscopy. Phys. Chem. Chem. Phys. 9 (11): 1276–1290.

[82] Graf D., Molitor F., Ensslin K., Stampfer C., Jungen A., Hierold C., Wirtz L. (2007) Spatially resolved Raman spectroscopy of single- and few-layer graphene. Nano Lett. 7 (2), 238–242.

[83] Casiraghi C., Hartschuh A., Qian H., Piscanec S., Georgi C., Fasoli A., Novoselov K. S., Basko D. M., Ferrari A. C. (2009) Raman spectroscopy of graphene edges. Nano Lett. 9 (4): 1433–1441.

[84] Casiraghi C., Pisana S., Novoselov K. S., Geim A. K., Ferrari A. C. (2007) Raman fingerprint of charged impurities in graphene. Appl. Phys. Lett. 91 (23): 233108–233110.

[85] Tommasini M., Castiglioni C., Zerbi G., Barbon A., Brustolon M. (2011) A joint Raman and EPR spectroscopic study on ball-milled nanographites. Chem. Phys. Lett. 516 (4): 220–224.

[86] Amarnath C. A., Hong C. E., Kim N. H., Ku B. C., Kuila T., Lee J. H. (2011) Efficient synthesis of graphene sheets using pyrrole as a reducing agent. Carbon 49 (11): 3497–3502.

[87] Galimberti M., Barbera V., Citterio A., Sebastiano R., Valerio A. M., Leonardi G. (2015) Adducts between carbon allotropes and serinol derivatives. WO2015EP72641.

[88] Galimberti M., Barbera V., Cipolletti V., Guerra S., Citterio A. (October 14 2014) Innovative biosourced compatibilizers for carbon and white fillers in rubber compounds. *Presented at the Fall 186th Technical Meeting of the Rubber Division of the American Chemical Society, Inc.* Nashville (TN). 16.

[89] Galimberti M., Barbera V., Truscello A., Sebastiano R., Valerio A. M. (2016) Polymer comprising repeating units consisting of a substituted pyrrole ring and products obtained by combining said polymers with carbon allotropes. WO2016023915 A1.

[90] Bahnmueller S., Meyer H., Dijkstra D., Henning W., Koning C. E., Van S. Y. H., Mulders S. F. M. (2010) Polyurethane compounds having carbon nanotubes. WO2010102763 A1.

[91] Barlow F.W. (2001) Basic elastomer technology, chapter 9. 235-258. Eds. Rubber Division American Chemical Society, The University of Akron

[92] Natural Rubber Statistics 2016 [Internet]. Available from http://www.lgm.gov.my/nrstat/nrstats.pdf

[93] Potts J. R., Shankar O., Du L., Ruoff, R. S. (2012). Processing–morphology–property relationships and composite theory analysis of reduced graphene oxide/natural rubber nanocomposites. Macromolecules 45 (15): 6045–6055.

[94] Potts J. R., Shankar O., Murali S., Du L., Ruoff, R. S. (2013) Latex and two-roll mill processing of thermally-exfoliated graphite oxide/natural rubber nanocomposites. Compos. Sci. Technol. 74: 166–172.

[95] Luo Y., Zhao P., Yang Q., He D., Kong L., Peng Z. (2014) Fabrication of conductive elastic nanocomposites via framing intact interconnected graphene networks. Compos. Sci. Technol. 100: 143–151.

IntechOpen

IntechOpen

IntechOpen